

A model for $A = 3$ antinuclei production in proton-nucleus collisions

R.P. Duperray^a, K.V. Protasov^b, L. Derome^c, and M. Buénerd^d

Institut des Sciences Nucléaires, IN2P3-CNRS, UJFG, 53, Avenue des Martyrs, F-38026 Grenoble Cedex, France

Received: date / Revised version: date

Abstract. A simple coalescence model based on the same diagrammatic approach of antimatter production in hadronic collisions as used previously for antideuteron is used here for the hadroproduction of mass 3 antinuclei. It is shown that the model is able to reproduce the existing experimental data on \bar{t} and ${}^3\bar{\text{He}}$ production without any additional parameter.

PACS. 24.10.-i Nuclear-reaction models and methods

1 Introduction

The increasing interest in the study of production of light antinuclei in proton-proton and proton-nucleus collisions is motivated by the presence of anti-nuclei in cosmic rays which has potentially important implications on the matter-antimatter asymmetry of the universe. From this point of view, it is important to determine the amount of antimatter which can be produced in the galaxy through the interaction of high-energy protons with the interstellar gas. A new generation of experiments (AMS [1], PAMELA [2]) should be able to measure the flux of anti-matter in a near future.

The calculations of the \bar{t} and ${}^3\bar{\text{He}}$ production cross sections reported here are based on the same diagrammatic approach to the coalescence model as used recently [3] to describe the \bar{d} production in proton-proton and proton-nucleus collisions.

The coalescence model [4] is based on the simple hypothesis that the nucleons, produced during the collision of a beam and a target, fuse into light nuclei whenever the momentum of their relative motion is smaller than a coalescence radius p_0 in the momentum space, which is a free parameter of the model, usually fit to the experimental data (see [5] for example). A simple diagrammatic approach to the coalescence model developed in [6] provided a microscopic basis to the model. In this approach, the parameter p_0 is expressed in terms of the slope parameter of the inclusive nucleon production spectrum and of the wave function of the produced nucleus.

This diagrammatic approach has been generalized in [3] to antideuteron production by taking into account thresh-

old effects and the anisotropy of the angular distributions. This approach can reproduce most existing data without any additional parameter in energy domains where the inclusive antiproton production cross sections are well known.

This article reports on the application of this approach to the production of $A = 3$ antinuclei. It is the first microscopic calculation of this cross section to the knowledge of the authors. In [7], the ${}^3\bar{\text{He}}$ production cross section in proton-proton collisions was calculated using the standard coalescence model, with the parameter p_0 taken from the \bar{d} production data.

Unfortunately, the experimental data required to be compared to the calculations are limited. Only two sets of experiments have measured the production of mass 3 antinuclei in proton-nucleus collisions. \bar{t} and ${}^3\bar{\text{He}}$ were discovered at IHEP (Serpukhov), with one experimental point measured for \bar{t} and one for ${}^3\bar{\text{He}}$ [8,9], while in the CERN experiment (SPS, WA 33) [10,11], four experimental points were measured for \bar{t} and eight for ${}^3\bar{\text{He}}$. For these latter data however, the \bar{t} and ${}^3\bar{\text{He}}$ production cross sections were measured with respect to the pion production cross section at the same momentum. This requires the corresponding experimental values of the pion production cross section to be known to extract the values of the \bar{t} and ${}^3\bar{\text{He}}$ production cross sections.

The article is organized as follows. The main ideas of the theoretical approach are described in section 2. The formalism is generalized to the case of $A = 3$ antinuclei production in section 3. Section 4 is devoted to the results and the comparison to the experimental data. A brief summary of the work is provided before the work is concluded in the last section.

^a duperray@isn.in2p3.fr

^b protasov@isn.in2p3.fr

^c derome@isn.in2p3.fr

^d buenerd@isn.in2p3.fr

2 Diagrammatic approach to the coalescence model

The main ideas of the diagrammatic approach of the coalescence model for nuclear fragment production are reminded here for the reader's convenience [6]. The simplest Feynman diagram of Fig. 1 corresponding to fusion of three nucleons is considered as a basis for the coalescence model. Here the symbol f designates the state of all particles but nucleons 1, 2 and 3 which form the tritium or the helium 3 nucleus produced in the final state (specified by the t symbol on the graph).

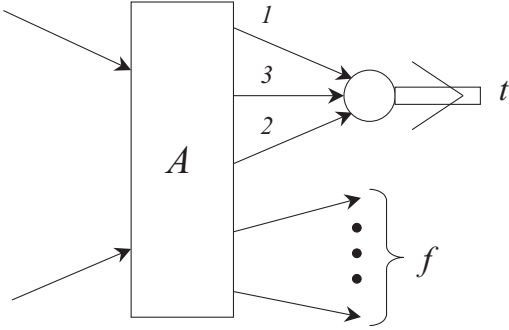


Fig. 1. The simplest Feynman diagram corresponding to coalescence of three nucleons into a tritium or ^3He .

The physical picture behind this diagram is quite simple: the nucleons produced in a collision (block A) are slightly virtual and can fuse without any further interaction with the nuclear field. This diagram is not the only possible contribution to the full transition amplitude. However, mutual cancellations of a number of other contributing diagrams result in the diagram of Fig. 1 being dominant [12]. This diagram can be calculated using the technique developed in [13].

The probability for three nucleon coalescence is given by:

$$d^3W_t = |M|^2 \frac{m_t}{E_t} \frac{d^3p_t}{(2\pi)^3}, \quad (1)$$

where m_t is the mass of the t fragment and E_t its energy in the (beam)nucleon-(target)nucleon center of mass system of the colliding nuclei. The probability for three nucleon production is then:

$$d^9W_{123} = |M_A|^2 \frac{m_p}{E_1} \frac{d^3p_1}{(2\pi)^3} \frac{m_p}{E_2} \frac{d^3p_2}{(2\pi)^3} \frac{m_p}{E_3} \frac{d^3p_3}{(2\pi)^3}, \quad (2)$$

where M_A is the amplitude corresponding to the block A, i.e., accounting for the inclusive production of nucleons 1, 2 and 3 and other particles in the final state f . To avoid cumbersome expressions in equations (1) and (2), the factors corresponding to colliding nuclei have been omitted

since they cancel in further calculations. Using the conventional graph technique [13], the expression for M can be written in the form:

$$M = \int \frac{d^4p_1}{(2\pi)^4} \int \frac{d^4p_2}{(2\pi)^4} \int \frac{d^4p_3}{(2\pi)^4} \frac{2m_p}{m_p^2 - p_1^2 - i0} \frac{2m_p}{m_p^2 - p_2^2 - i0} \frac{2m_p}{m_p^2 - p_3^2 - i0} i(2\pi)^4 \delta^4(p_1 + p_2 + p_3 - p_t) M_{(1,2,3 \rightarrow t)} M_A \quad (3)$$

where $M_{(1,2,3 \rightarrow t)}$ is the vertex of coalescence of 1,2,3 into t (proportional to the three-nucleon wave function in the momentum space in the nonrelativistic approximation), m_p the nucleon mass, the three fractions being the individual nucleon propagators of 1, 2 and 3. The integrals have to be performed over energies and momenta of the (virtual) particles. The delta functions ensure energy-momentum conservation at the t vertex, $p_t = (\mathbf{p}_t, E_t)$, with $\mathbf{p}_t = \mathbf{p}_1 + \mathbf{p}_2 + \mathbf{p}_3$ being the momentum of t , E_t its energy. The dependence of the amplitude M_A on its variables (the particle momenta) is also needed explicitly for the calculations. In lack of a reliable theoretical form, this can be done in a "minimal" way, by using empirical shapes. The inclusive nucleon spectra usually have a decreasing form which can be approximated by a Gaussian function in the center of mass frame:

$$E_p \frac{d^3\sigma_p}{dp_p^3} \propto \exp(-\mathbf{p}_p^2/Q^2), \quad (4)$$

where Q defines the slope parameter of the momentum distribution. Accordingly, the amplitude M_A can be written in the following way:

$$M_A = C \exp\left(-\frac{\mathbf{p}_1^2 + \mathbf{p}_2^2 + \mathbf{p}_3^2}{2Q^2}\right) = C \exp\left(-\frac{\mathbf{p}_t^2}{6Q^2}\right) \exp\left(-\frac{\mathbf{q}^2}{Q^2}\right) \exp\left(-\frac{3\mathbf{p}^2}{4Q^2}\right), \quad (5)$$

where

$$\begin{aligned} \mathbf{p}_t &= \mathbf{p}_1 + \mathbf{p}_2 + \mathbf{p}_3, \\ \mathbf{p} &= \frac{1}{\sqrt{3}}(\mathbf{p}_1 - \mathbf{p}_2), \\ \mathbf{q} &= \frac{1}{2\sqrt{3}}(\mathbf{p}_1 + \mathbf{p}_2 - 2\mathbf{p}_3). \end{aligned} \quad (6)$$

Assuming a statistical independence in the three nucleon production process, the inclusive production cross section can be written as the product of the three independent probabilities:

$$\frac{d^9W_{123}}{dp_1^3 dp_2^3 dp_3^3} = \frac{1}{\sigma_{inel}^2} \frac{d^3W_1}{dp_1^3} \frac{d^3W_2}{dp_2^3} \frac{d^3W_3}{dp_3^3}, \quad (7)$$

where σ_{inel} is the total reaction cross-section of the colliding particles.

After integration of (3), taking into account (5) and (7), and dividing by the incident particle flux, the t production cross section takes the form:

$$E_t \frac{d^3\sigma_t}{dp_t^3} = \frac{96\pi^6}{m_p^2\sigma_{inel}^2} |S|^2 E_1 \frac{d^3\sigma_1}{dp_1^3} E_2 \frac{d^3\sigma_2}{dp_2^3} E_3 \frac{d^3\sigma_3}{dp_3^3}, \quad (8)$$

with $\mathbf{p}_1 = \mathbf{p}_2 = \mathbf{p}_3$, $\mathbf{p}_t = 3\mathbf{p}_1$ and

$$S = \int \exp\left(-\frac{\mathbf{q}^2}{Q^2} - \frac{3}{4}\frac{\mathbf{p}^2}{Q^2}\right) \Psi_t(\mathbf{p}, \mathbf{q}) \frac{d^3\mathbf{p}}{(2\pi)^3} \frac{d^3\mathbf{q}}{(2\pi)^3}. \quad (9)$$

Where $\Psi_t(\mathbf{p}, \mathbf{q}) \propto M_{123 \rightarrow t}$ is the wave function of the t (or ${}^3\text{He}$) system normalized by the condition

$$\int |\Psi_t(\mathbf{p}, \mathbf{q})|^2 \frac{d^3\mathbf{p}}{(2\pi)^3} \frac{d^3\mathbf{q}}{(2\pi)^3} = 1. \quad (10)$$

The factor $1/2$, accounts for nucleons and $A = 3$ nuclei spins, is included in (8). The three-nucleon wave function is needed at sufficiently large momenta to compute the amplitude. The wave function of [14] has been used (see appendix for discussion).

The structure of (8) is the same as that of the coalescence model and the S integral in 8 can be straightforwardly related to the coalescence momentum:

$$p_0^3 = 18\sqrt{3}\pi^2 \int \frac{d^3\mathbf{p}}{(2\pi)^3} \frac{d^3\mathbf{q}}{(2\pi)^3} \exp\left(-\frac{\mathbf{q}^2}{Q^2} - \frac{3}{4}\frac{\mathbf{p}^2}{Q^2}\right) \Psi_t(\mathbf{p}, \mathbf{q}). \quad (11)$$

Thus, in the approach based on the diagram of Fig. 1 and within the approximations made above, the coalescence momentum p_0 is not an adjustable parameter anymore, but it is determined by the inclusive proton spectrum and by the trinucleon wave function. Note that in that case, p_0 depends on the momentum distribution and should thus be energy and system dependent.

3 Application to three-antinuclei production

In order to generalize the diagrammatic approach of the coalescence model to the production of $A = 3$ antinuclei (noted \bar{t} further below), two effects have to be taken into account: the anisotropy of angular distributions and the threshold effects [3]. Isotropic angular dependence are frequently assumed in nonrelativistic collisions. However, in relativistic collisions, the momentum distributions are strongly anisotropic and the low energy approximation cannot be used. To take this into account, formula (8) can be easily generalized to any angular dependence. Assuming the inclusive nucleon production cross section to be given by the (parameterized) amplitude $M_1(\mathbf{p}_1)$:

$$E_1 \frac{d^3\sigma_1}{dp_1^3} = |M_1(\mathbf{p}_1)|^2, \quad (12)$$

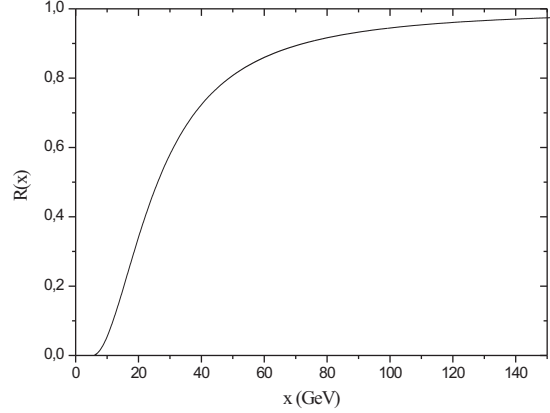


Fig. 2. Dependence of the threshold factor $R(x)$, with x as defined in the text.

The cross section for t production can then be written (see 8):

$$E_t \frac{d^3\sigma_t}{dp_t^3} = \frac{96\pi^6}{m_p^2\sigma_{inel}^2} \left[\int M_1(\mathbf{p}_1) M_2(\mathbf{p}_2) M_3(\mathbf{p}_3) \Psi_t(\mathbf{p}, \mathbf{q}) \frac{d^3\mathbf{p}}{(2\pi)^3} \frac{d^3\mathbf{q}}{(2\pi)^3} \right]^2. \quad (13)$$

This model could be practically used directly to describe the production of \bar{t} . The production threshold of the antiparticle has to be taken into account however in the cross section calculation. The same procedure to evaluate the cross section near threshold as that used in [3] will be applied here. In nucleon-nucleon collisions, the main reaction producing a \bar{t} particle is $NN \rightarrow \bar{t} + 5N$. Near the threshold of this reaction, the energy dependence of the \bar{t} production cross section is mostly governed by the five nucleons phase space: $\Phi(\sqrt{s + m_t^2 - 2\sqrt{s}E_{\bar{t}}}; 5m_p)$,

$$E_{\bar{t}} \frac{d^3\sigma_{\bar{t}}}{dp_{\bar{t}}^3} \propto \Phi(\sqrt{s + m_t^2 - 2\sqrt{s}E_{\bar{t}}}; 5m_p). \quad (14)$$

The phase space Φ for n particles with masses, momenta and energies, m_i , \mathbf{p}_i , and E_i respectively, is defined in the usual way (in the center of mass)

$$\Phi(\sqrt{s}; m_1, m_2, \dots, m_n) = \prod_{i=1}^n \frac{1}{(2\pi)^3} \frac{d^3p_i}{2E_i} \delta^3\left(\sum_{i=1}^n \mathbf{p}_i\right) \delta\left(\sum_{i=1}^n E_i - \sqrt{s}\right).$$

It was calculated here by using the standard CERN library program (W515, subroutine GENBOD) [15]. \sqrt{s} is the total energy of the n particles in the center of mass system.

A phenomenological correction factor R can thus be introduced in formulae (13) which then reads:

$$R(x) = \frac{\Phi(x; 5m_p)}{\Phi(x; 5 \times 0)}, \quad (15)$$

where $x = \sqrt{s + m_t^2 - 2\sqrt{s}E_t}$, and where the denominator contains the high energy limit of the phase space to ensure R to be dimensionless and to do not change the value of the cross section out of the space phase boundary. The limits of R are thus:

$$R \rightarrow 0, \quad E_t \rightarrow E_t^{\max} = \left(\frac{s + m_t^2 - (5m_p)^2}{2\sqrt{s}} - m_t \right),$$

$$R \rightarrow 1, \quad \sqrt{s} \rightarrow \infty.$$

If $p_t^2 \ll (\sqrt{s} - E_t)^2$, the expression $\sqrt{s + m_t^2 - 2\sqrt{s}E_t}$ can be replaced by $\sqrt{s} - E_t$. This same approximation was made in [3]. The functional dependence of $R(x)$ is shown in Fig. 2.

4 Results on antinuclei production data

4.1 Status of the data

This section is introduced with a brief overview of the current experimental situation on the antinuclei production relevant to the present study, i.e., in proton-proton and proton-nucleus collisions. The antinuclei production in ion-ion collisions will be quoted only for completeness.

- As mentioned in the introduction, the experimental data on the production of mass 3 antinuclei are extremely scarce, and much less informative than that on antideuteron production, with only two experiments or sets of experiments reporting on mass 3 antinuclei production in proton-nucleus collisions [8,9,10,11]. Note that there are no experimental data available on the production of these antinuclei in proton-proton collisions. The production of ${}^3\bar{\text{He}}$ has been observed recently in various heavy ion studies like $Pb + Pb$ collisions at ultra relativistic incident energies [16]. These data are out of the scope of the present work. They will not be discussed here (see [3] for a discussion).
- Coalescence calculations require the antiproton production cross section to be known for antiproton momenta equal to approximately one third of the $A = 3$ antinuclei momenta. Unfortunately, in most experiments the differential cross sections for antiproton and $A = 3$ antinuclei productions were not measured at this momentum. The \bar{p} cross section thus had to be extrapolated to the appropriate kinematical region when no other data were available, which of course, introduces additional uncertainty in the calculations.

The three nucleon wave functions needed in the calculations are much less well known than the deuteron wave function. In addition, the same wave function will be used for ${}^3\text{He}$ and t nuclei (see appendix). The inaccuracy on the tri-nucleon wave functions is thus another source of uncertainty.

The total reaction cross-section used in the calculations was described by means of the parameterization proposed in [17].

4.2 Proton Aluminium collision data at 70GeV/c

The antinuclei produced in the Serpukhov experiments [8, 9] were obtained from a 70 GeV/c proton beam incident on an aluminium target at 27 mrad scattering angles and 20 GeV/c for ${}^3\bar{\text{He}}$, and 0 and 25 GeV/c for \bar{t} . The inclusive antiproton cross sections were available from [18] and [19] in the same kinematical conditions.

In Fig. 3 the \bar{p} cross section data from [8] are compared with the results of fits using a functional form [20]. The solid curve corresponds to a fit of a large sample of $p + A \rightarrow \bar{p}$ data from 12 up to 400 GeV incident energies not including those from reference [8] which were found not to be compatible with the other sets of data [20]. The calculated values are in fair agreement with the two lowest momentum data points (which were obtained by extrapolation from measurements at other angles). They overestimate the other data points by a factor of 2 to 4. The dotted curve is a renormalization of the solid curve by a factor ≈ 2.5 to fit these latter points, while the dashed curve corresponds to the fit of the single set of data points shown on the figure, which parameters however give quite poor agreement with the other sets of data [20].

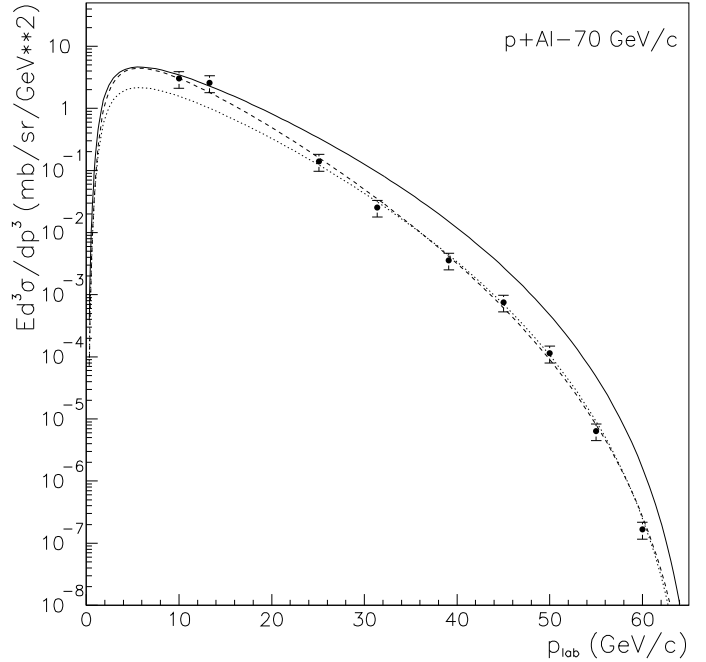


Fig. 3. Inclusive differential cross section for antiproton production in p+Al collisions as a function of the total momentum in the laboratory frame from [8], compared to calculated values as discussed in the text.

It must be emphasized that the low momentum region, say $p_{lab} < 10$ GeV/c, which is the useful region for the coalescence calculations, with $\mathbf{p}_{\bar{p}} \approx \mathbf{p}_{\bar{t}}/3$ is particularly important here, with unfortunately no data point from direct measurement available over the relevant range.

Fig. 4 compares the calculations for the $A = 3$ production cross section for the three parameterizations shown

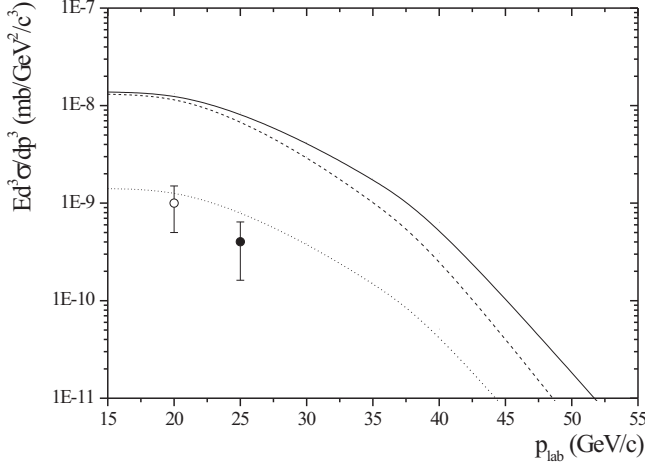


Fig. 4. The inclusive differential cross-section for \bar{t} [8] (open circles) and ${}^3\text{He}$ [9] (black circles) production by 70 GeV protons on Al target as a function of the total momentum in the laboratory frame compared to calculations using the microscopic model of coalescence and the same three different parameterizations of the antiproton production cross-section as shown on figure 3, with the same graphical conventions.

on Fig. 3 with the experimental data. The calculations using the global fit renormalized to the 70 GeV/c data (see Fig. 3) give by far the best agreement with the \bar{t} data (dotted curve). The other two sets of \bar{p} cross section parameters overestimate the data by a sound order of magnitude. This is apparently consistent with the larger \bar{p} cross section predicted by these two sets of parameters for low \bar{p} momentum region to which the \bar{t} cross section is most sensitive. The factor of about 2 between the \bar{p} cross sections predicted by the two groups of parameters translates into a factor of about 10 for the \bar{t} cross section because of the approximately cubic dependence of the latter on the \bar{p} cross section. However it is somewhat puzzling that this agreement is obtained with parameters which are not consistent with the whole body of \bar{p} data [20].

4.3 Proton beryllium collision data at 200 GeV/c

In the CERN experiments [10,11], \bar{p} , \bar{t} and ${}^3\text{He}$ were produced in proton-beryllium collisions at 200, 210, and 240 GeV/c and detected at 0 degree scattering angle [11], while \bar{p} were measured at 200 GeV/c [10] on the same targets. For these data however, the production cross sections were measured as the ratios to the π^- production cross sections at the same momentum. The knowledge of the corresponding experimental π^- production cross section, or a good parameterisation of the latter, is thus required in order to allow the values of the \bar{p} , \bar{t} and ${}^3\text{He}$ production cross sections to be calculated.

Fortunately, the $p + Be \rightarrow \pi^- + X$ cross section has been measured at 200 and 300 GeV/c incident momentum in [21] in similar kinematical conditions as in the CERN

parameter	C_1	C_2	C_3	C_4
value	0.94	1.88	7.05	1.69

Table 1. Values of the parameters of relation 16 obtained by fitting the π^- production cross sections for 200 and 300 GeV/c protons on Beryllium.

experiment. The measured distributions have been fit by means of the following functional form, inspired from ref [22]:

$$E \frac{d^3 \sigma}{dp^3} (\pi^-) = C_1 \sigma_{in} (1-x)^{C_2} e^{-C_3 x} e^{-C_5 p_\perp}, \quad (16)$$

where $x = E^-/E_{max}^*$ (E^* is the total energy of the inclusive particle in the center of mass frame, σ_{in} is the total reaction cross section for the system in collision, \sqrt{s} is the total energy of the system and p_\perp the transverse momentum of the emitted particle. The values of the parameters obtained are given in Table 1 and the results of this fit are presented in Fig. 5. The parameterization (16) has been

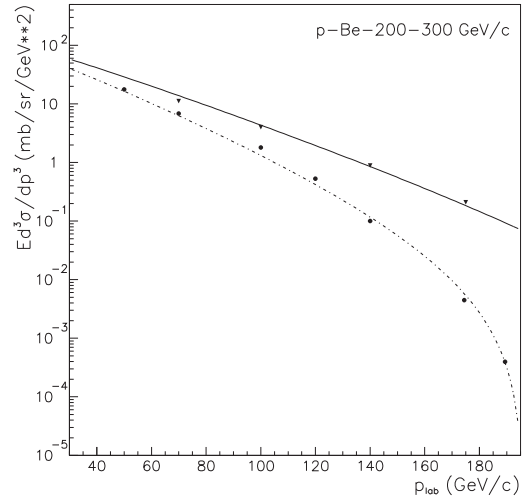


Fig. 5. Experimental inclusive differential cross-section for π^- production in $p + Be$ collisions [21] (symbols) at 200 GeV/c (full circles) and 300 GeV/c (full triangles) compared with the functional form 16.

used to extract the experimental \bar{p} production cross sections [10]. The resulting cross section values are compared in Fig. 6 with the results of the fit of a functional form to a large sample of $p + A \rightarrow \bar{p} + X$ data from 12 GeV/c up to 400 GeV/c incident momenta [20]. It is seen that the data points derived previously and the calculated values are in fair agreement. This consistency gives confidence to the following steps of the analysis for the evaluation of the \bar{t} and ${}^3\text{He}$ production cross sections. In Fig. 7, the \bar{t} and ${}^3\text{He}$ production cross sections are compared to

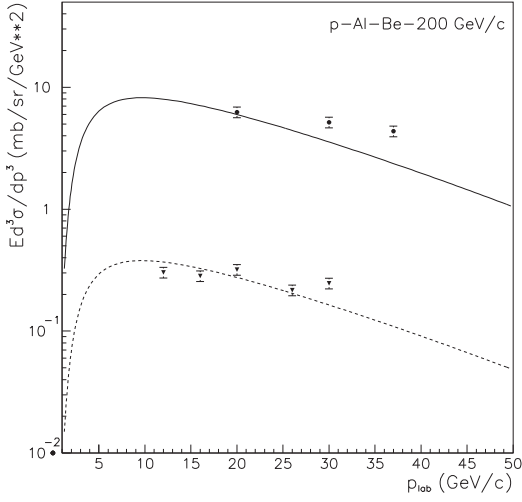


Fig. 6. Experimental inclusive differential cross-sections for \bar{p} production in $p + Al$ collision (circles), and in $p + Be$ collision ($\times 10^{-1}$, triangles), [18] compared with the results of fits using a functional form (curves) [20].

calculations using the microscopic model of coalescence. The agreement between experimental and calculated values varies from poor to good. On the average however data and calculations are within one order of magnitude. This result should be considered as a success in account of the numerous sources of uncertainties of the calculations and of the limited accuracy of the measurements. Note also that refs [10] and [11] report experimental values in disagreement by a factor of 2. Furthermore the \bar{t} and ${}^3\text{He}$ production cross section, measured at the same momentum, should be in principle close to each other (this fact is clearly seen in the same experiment for t and ${}^3\text{He}$ production) whereas, in this experiment, they are quite different.

5 Conclusion

It has been shown in this work that the diagrammatic approach to the coalescence model developed previously can successfully account for the mass 3 antinuclei production cross section in proton-nucleus collisions over wide kinematical conditions without any additional parameter. These calculations require a good knowledge of the antiproton production cross-section and of the three-nucleon wave function. These results would be further used to calculate \bar{t} and ${}^3\text{He}$ flux in cosmic rays.

Appendix

In this appendix, we briefly remind how the wave functions of the trinucleon is written in [14], while in this paper slightly different definitions have been used. A useful analytical parameterization of the bound trinucleon wave

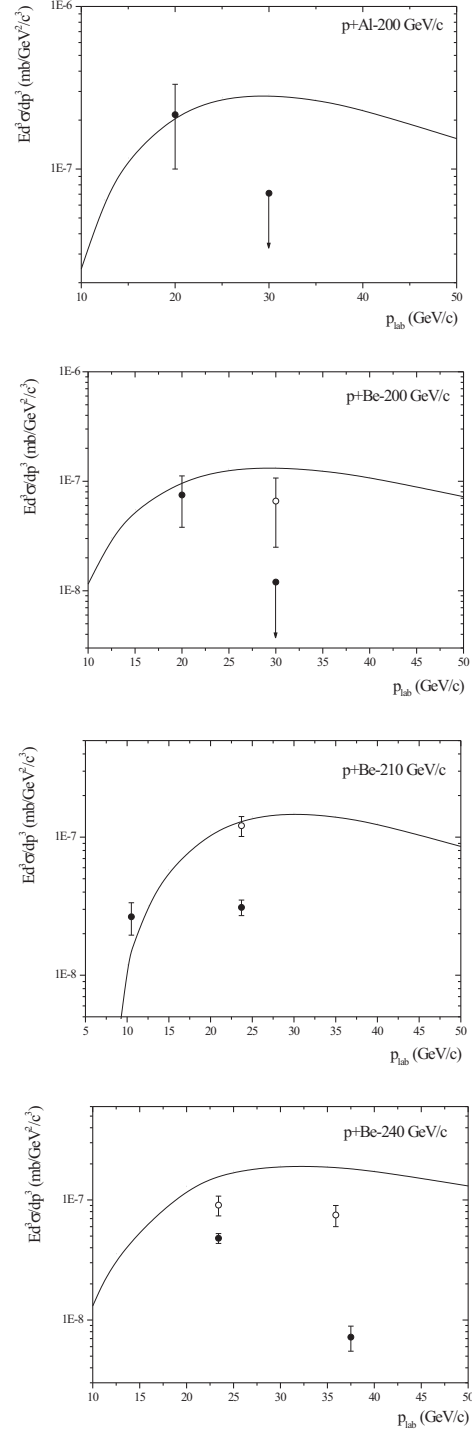


Fig. 7. Experimental inclusive differential cross-section for \bar{t} (full circles) and ${}^3\text{He}$ (open circles) production in $p + Al$ and $p + Be$ collisions, compared to calculations using the microscopic model of coalescence (solid line).

function is obtained from solving the Faddeev equation with the Reid soft-core potential.

The total wave function of the triton is written as a sum of 3 Faddeev components

$$\Psi = \sum_{i=1}^3 \Psi_t^i(\mathbf{q}_i, \mathbf{p}_i).$$

In (9)-(13), we make use of only one Faddeev component Ψ_t , while due the exchange symmetry of two-nucleons in the triton, all the three Faddeev components are identical. Furthermore, Faddeev components Ψ_t are decomposed in terms of their partial wave components with respect to the spin-isospin and angular momentum basis $\phi_\alpha(\hat{\mathbf{p}}, \hat{\mathbf{q}})$.

$$\Psi_t(\mathbf{p}, \mathbf{q}) = \sum_{\alpha} \psi_{\alpha}(p, q) \phi_{\alpha}(\hat{\mathbf{p}}, \hat{\mathbf{q}}),$$

with, if \mathbf{p}_i ($i = 1, 2, 3$) is the nucleon momenta

$$\mathbf{p} = \frac{1}{2}(\mathbf{p}_1 - \mathbf{p}_2), \mathbf{q} = \frac{1}{2\sqrt{3}}(\mathbf{p}_1 + \mathbf{p}_2 - 2\mathbf{p}_3).$$

The following normalization is used

$$\int |\Psi_t(\mathbf{p}, \mathbf{q})|^2 d^3\mathbf{p} d^3\mathbf{q} = \sum_{\alpha} \int dp dq p^2 q^2 |\psi_{\alpha}(p, q)|^2 = 1.$$

Note that, in these expressions, the definition of \mathbf{p} and the normalization differ from (6) and (10). Ψ_t is a sum of the partial wave state α which is a label for the following physical quantities:

- L , the angular momentum of the pair of nucleons (1-2).
- l , the angular momentum of nucleon 3 according to the center of the mass of the pair of nucleons (1-2).
- \mathcal{L} , the total angular momentum of the triton.
- s , the spin of the pair of nucleons (1-2).
- \mathcal{S} , the total spin of the triton.
- T , the isospin of the pair of nucleons (1-2).

Only two components label α were taken into account, $\alpha = 1, 2$.

- For $\alpha = 1$, $L = l = \mathcal{L} = 0$, $s = 1$, $\mathcal{S} = 1/2$ and $T = 0$.
- For $\alpha = 2$, $L = l = \mathcal{L} = s = 0$, $\mathcal{S} = 1/2$ and $T = 1$.

Of course, the fact to consider only two partial wave state is an approximation which gives the probability of 89.25% of trinucleon being in the partial wave state α . In [14], the parameterization for $\psi_{\alpha}(p, q)$ is given by

$$\psi_{\alpha}(p, q) = p^L p^l (p^2 + \Omega_{p1}^2)^{-1} \prod_{m=1}^3 (q^2 + \Omega_{qm}^2)^{-1} \sum_{i=1}^6 \sum_{j=1}^6 \frac{C_{ij}}{(p^2 + \mu_i^2)(q^2 + \nu_j^2)},$$

with Ω_{p1} , Ω_{qm} , μ_i , ν_j and C_{ij} all depending on the partial wave label α . The numerical values of these coefficients can be found in [14].

${}^3\text{He}(ppn)$ and $t(pnn)$ are considered to have the same wave function. Although, because of the presence of the Coulomb interaction, these two wave functions are slightly different, this difference is negligible compared to the other uncertainties of present calculations.

References

1. See section IV in Nucl. Phys. B (Proc. Suppl.) 113(2002).
2. O. Adrani et al., Nucl. Instr. Meth. **A478**, 114 (2002).
3. R.P. Duperray, K.V. Protasov, A.Yu. Voronin, Eur. Phys. J., **A16**, 27 (2003)
4. S.T. Butler and C.A. Pearson, Phys. Rev. Lett. **7**, 69 (1961); Phys. Lett. **1**, 77 (1962); Phys. Rev. **129**, 836 (1963); A. Schwarzschild and C. Zupancic, Phys. Rev. **129**, 854 (1963); L.P. Csernai and J.I. Kapusta, Phys. Rep. **131**, 223 (1985).
5. See for example the classical paper S. Nagamya et al., Phys. Rev. **C24** 971 (1981) and Nucl. Phys. **A661** (1999) for recent references.
6. V.M. Kolybasov, Yu.N. Sokol'skikh, Phys. Lett. **B225**, 31 (1989); Sov. J. Nucl. Phys. **55**, 1148 (1992).
7. P. Chardonnet, J. Orloff, P. Salati, Phys. Lett. **B409**, 313 (1997).
8. Y.M. Antipov et al., Phys. Lett. **B34**, 164(1971).
9. N.K. Vishnevskii et al., Sov. J. Nucl. Phys. **20**, 371 (1974).
10. W. Bozzoli et al., Nucl. Phys. **B144**, 317(1978).
11. A. Bussière et al., Nucl. Phys. **B174**, 1(1980).
12. M.A. Braun and V.V. Vechernin, Sov. J. Nucl. Phys. **44**, 506 (1986); **36**, 357 (1982).
13. I.S. Shapiro, *Dispersion theory of direct nuclear reactions*, in *Selected Topics in Nuclear Theory*, Ed. F. Janouch, IAEA, Vienna, 1963; I.S. Shapiro, Usp. Fiz. Nauk. **92**, 549 (1967) [Sov. Phys. Usp. **10**, 515 (1968)].
14. Muslim and Y.E.kim Nucl. Phys. **A427**, 235 (1984).
15. F. James, Monte Carlo Phase Space, CERN 68-15 (1968); <http://wwwinfo.cern.ch/asdoc/shortwrupsdir/w515/top.html>
16. G. Appelquist et al., Phys. Lett. **B376**, 245(1996), see Nucl. Phys A661,1999 for more on this issue.
17. J.R. Letaw, R. Silberberg, and C.H. Tsao, Ap.J.Suppl. **51** 271 (1983)
18. F. Binon et al., Phys. Lett. **30B**, 510(1969).
19. Yu.B. Bushnin et al., Sov. J. Nucl. Phys. **10**, 337 (1970).
20. R.P. Duperray, C.Y. Huang, K.V. Protasov and M.Buénér, in preparation.
21. W.F. Baker et al., Phys. Lett. **51B** 303 (1974)
22. A.N. Kalinovskii, N.V. Mokhov and Yu.P. Nikitin, *Passage of high-energy particles through matter*, American Institute of Physics, New York (1989).